Int. J. Solids Structures Vol. 22 No. 3, pp. 307–314, 1986
Printed in Great Britain

0020–7683/86 $3.00 + .00

THERMAL AND RESIDUAL STRESSES OF CZOCHRALSKI-GROWN SEMICONDUCTING MATERIAL

TOSHIHIRO IWAKI† and NOBUYUKI KOBAYASHI‡
Faculty of Engineering, Toyama University, Toyama 930, Japan

(*Received* 28 *February* 1985; *in revised form* 22 *April* 1985)

Abstract—The thermal stresses during pulling and the residual stresses after pulling in a Czochralski-grown semiconducting crystal are obtained analytically by using an isotropic thermoelastic model. It is assumed that a finite cylindrical crystal is withdrawn from a melt with a constant pulling rate, and the physical properties of crystal are independent of temperature. Moreover the problem is considered to be a quasi-stationary one. Numerical results show that the Biot number is a prime factor affecting the thermal and residual stresses. The differences between the models of the finite crystal and semi-infinite crystal are described. An explanation of the experimental results is attempted.

INTRODUCTION

Single crystals of Si, GaAs, and InP are typical materials for the current semiconductor device technology. They are usually produced by Czochralski pulling, which is one of the most standard crystal growth techniques[1]. Dislocation-free crystals are strongly desired because the dislocation deteriorates electrical and optical qualities of the crystal[1]. It is known that dislocations are primarily produced by the thermal stress. Therefore, growth conditions facilitating the reduction of the thermal stress and consequently of dislocations are required.

Billig[2] and Tsivinsky[3] attempted to explain dislocations by the thermal stress produced only by the radial temperature drop. Penning[4], Avdonin *et al.*[5], Brice [6] and Jordan *et al.*[7] studied the thermal stress in the crystal under the plane strain assumption by using an isotropic thermoelastic theory. The plane strain theory, which is guaranteed only if the temperature is independent of the axial distance, is not satisfied because an axial temperature gradient arises in the crystal. Furthermore, they did not consider that the stress components vanish at the growing interface. Therefore, their results are not valid for the thermal stress in the growing crystal. Iwaki and Kobayashi[8] presented an analytical solution for the thermal and residual stresses in a semi-infinite cylindrical crystal with a planar solid–liquid interface. It was concluded that the Biot number was a prime factor affecting the thermal and residual stresses. However, the thermal stress at the early stage of crystal pulling process was not yet considered.

The thermal stress is very sensitive to material geometry. The length of the crystals of GaAs and InP is presently about twice their radius. The purpose of this paper is to obtain the thermal stresses in a finite crystal and to compare them with those of a semi-infinite crystal. An explanation for experimental results obtained by Jordan *et al.*[7], Shimada *et al.*[9] and Chen and Holmes[10] is attempted.

STATEMENT OF PROBLEM

The Czochralski-grown crystal, which has a circular cylindrical shape with a radius a, a finite length vt and planar ends, is withdrawn with a constant pulling rate v, where t is time (Fig. 1). At the cylindrical side surface and the top end of the crystal, heat is transferred by Newton's law of cooling, and at the bottom end the temperature is at

† Lecturer. Author to whom correspondence should be addressed.
‡ Professor.

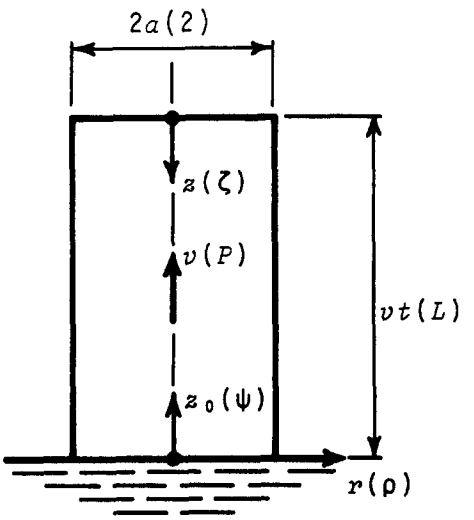

Fig 1. Present model.

the melting point T_m. It is assumed that thermal conductivity k and thermal diffusivity κ are constant, and the temperature variations T in the crystal with time are slow. Jordan *et al.* obtained the quasi-steady-state (QSS) solution and showed that their QSS assumption is satisfactory[7]. Following their assumption, we treat the problem as a quasi-stationary one for mathematical simplicity. On the assumption that modulus of elasticity E, Poisson's ratio ν and coefficient of thermal expansion α are constant and a stress-free layer is formed at the bottom end as the crystal grows, the thermal stresses during pulling and the residual stresses after pulling are obtained by using isotropic thermoelastic theory.

STRESS FIELD

By cylindrical symmetry with respect to the z-axis, the Fourier heat-conduction equation in the dimensionless form is expressed by [8]

$$\Delta^* T^* = P(\partial T^*/\partial\psi), \tag{1}$$

where

$$\Delta^* = \frac{\partial^2}{\partial\rho^2} + \frac{1}{\rho}\frac{\partial}{\partial\rho} + \frac{\partial^2}{\partial\psi^2};$$

$$\rho = \frac{r}{a}; \quad \psi = \frac{z_0}{a} = -\zeta + L; \quad \zeta = \frac{z}{a}; \quad L = \frac{vt}{a};$$

$$T^* = \frac{T - T_a}{T_m - T_a}; \quad P = \frac{av}{\kappa}$$

is the Peclet number, and T_a is a temperature of environment. The boundary conditions are

$$T^* = 1 \quad (\psi = 0), \tag{2a}$$

$$(\partial T^*/\partial\rho) + BT^* = 0 \quad (\rho = 1), \tag{2b}$$

$$(\partial T^*/\partial\psi) + BT^* = 0 \quad (\psi = L), \tag{2c}$$

where $B = ah/k$ is the Biot number, and h is a convective heat transfer coefficient.

With the usual technique of separation of variables we find the solution of eqn (1) subjected to the boundary conditions (2):

$$T^* = \sum_{n=1}^{\infty} (A_n e^{q\psi} + \bar{A}_n e^{\bar{q}\psi}) J_0(\alpha_n \rho), \tag{3}$$

where α_n is the nth root of the transcendental equation

$$\alpha J_1(\alpha) - B J_0(\alpha) = 0, \tag{4}$$

and

$$q = q(\beta_n) = P/2 - \beta_n, \tag{5a}$$

$$\bar{q} = q(-\beta_n), \tag{5b}$$

$$A_n = A_n(\beta_n) = \frac{(\beta_n + D)e^{\beta_n L}}{(\alpha_n^2 + B^2) J_0(\alpha_n)(D \sinh \beta_n L + \beta_n \cosh \beta_n L)}, \tag{5c}$$

$$\bar{A}_n = A_n(-\beta_n), \tag{5d}$$

where $\beta_n = \{\alpha_n^2 + (P/2)^2\}^{1/2}$; $D = B + P/2$, and $J_0(x)$ and $J_1(x)$ are Bessel functions of the first kind of orders zero and one, respectively.

The displacement potential ϕ_0^* and the Love stress function ϕ_l^*, which are introduced in order to find the stresses induced by a temperature distribution T^*, have to satisfy the following equations, respectively:

$$\Delta^* \phi_0^* = T^* \tag{6}$$

and

$$\Delta^* \Delta^* \phi_l^* = 0. \tag{7}$$

The stress components derived from ϕ_0^* and ϕ_l^* are shown in eqns (11) and (12) in ref. [8]. Here the stress components σ_{ij} are defined by the dimensionless form $\sigma_{ij}^* = \sigma_{ij}(1 - \nu)/\{(T_m - T_a)\alpha E\}$ $(i, j = \rho, \theta, \psi)$.

The boundary conditions are

$$\sigma_{\rho\rho}^* = \sigma_{\rho\psi}^* = 0 \qquad (\rho = 1), \tag{8a}$$

$$\sigma_{\psi\psi}^* = \sigma_{\rho\psi}^* = 0 \qquad (\psi = 0 \text{ and } \psi = L). \tag{8b}$$

Substituting eqn (3) into eqn (6), we have a particular solution

$$\phi_0^* = \sum_{n=1}^{\infty} \{B_n e^{q\psi} + \bar{B}_n e^{\bar{q}\psi}\} J_0(\alpha_n \rho), \tag{9}$$

where

$$B_n = A_n/(q^2 - \alpha_n^2), \tag{10a}$$

$$\bar{B}_n = \bar{A}_n/(\bar{q}^2 - \alpha_n^2). \tag{10b}$$

The stress function ϕ_l^* is constructed in the form

$$\phi_l^* = \phi_1^* + \phi_2^*, \tag{11}$$

and the stresses σ_{1ij}^* and σ_{2ij}^* are derived from ϕ_1^* and ϕ_2^*, respectively.

A solution of ϕ_1^* becomes

$$\phi_1^* = \sum_{n=1}^{\infty} \{C_n e^{q\psi} J_0(q\rho) + D_n e^{q\psi} \rho J_1(q\rho) + \bar{C}_n e^{\bar{q}\psi} J_0(\bar{q}\rho) + \bar{D}_n e^{\bar{q}\psi} \rho J_1(\bar{q}\rho)\}. \quad (12)$$

The unknown coefficients C_n, $\bar{C}_n$, D_n and $\bar{D}_n$ are determined so as to satisfy the boundary conditions at the cylindrical surface:

$$\sigma_{0\rho\rho}^* + \sigma_{1\rho\rho}^* = 0 \qquad (\rho = 1), \quad (13a)$$

$$\sigma_{0\rho\psi}^* + \sigma_{1\rho\psi}^* = 0 \qquad (\rho = 1). \quad (13b)$$

Consequently, we have

$$C_n = B_n \Gamma(q), \quad (14a)$$

$$D_n = B_n \Lambda(q), \quad (14b)$$

$$\bar{C}_n = \bar{B}_n \Gamma(\bar{q}), \quad (14c)$$

$$\bar{D}_n = \bar{B}_n \Lambda(\bar{q}), \quad (14d)$$

where

$$\Gamma(q) = \frac{\alpha_n J_1(\alpha_n)\{2(1-\nu)J_1(q) - q^2 J_1(q) + 2(1-\nu)qJ_0(q)\} - q^2 J_0(\alpha_n)\{2(1-\nu)J_1(q) + qJ_0(q)\}}{\{2(1-\nu) - q^2\}J_1^2(q) - q^2 J_0^2(q)}, \quad (15a)$$

$$\Lambda(q) = \frac{\alpha_n J_1(\alpha_n) J_0(q) - q J_0(\alpha_n) J_1(q)}{\{2(1-\nu) - q^2\}J_1^2(q) - q^2 J_0^2(q)}. \quad (15b)$$

To satisfy the boundary condition (8b), the stress function ϕ_2^* is taken in the following form:

$$\phi_2^* = Q e^{\lambda\psi} J_0(\lambda\rho) + R e^{\lambda\psi} \rho J_1(\lambda\rho). \quad (16)$$

The stresses which are derived from ϕ_2^* must satisfy the boundary conditions at the cylindrical surface:

$$\sigma_{2\rho\rho}^* = \sigma_{2\rho\psi}^* = 0 \qquad (\rho = 1). \quad (17)$$

Then we have

$$Q\{\lambda J_0(\lambda) - J_1(\lambda)\} + R\{(2\nu - 1)J_0(\lambda) + \lambda J_1(\lambda)\} = 0, \quad (18a)$$

$$Q\{-\lambda J_1(\lambda)\} + R\{2(1-\nu)J_1(\lambda) + \lambda J_0(\lambda)\} = 0. \quad (18b)$$

For the solution of eqn (18) to be nontrivial the determinant must be zero. Hence, λ is the root of the transcendental equation

$$\{\lambda^2 - 2(1-\nu)\}J_1^2(\lambda) + \lambda^2 J_0^2(\lambda) = 0. \quad (19)$$

This equation has an infinite number of complex roots. If the nth root is defined by λ_n whose real and imaginary parts are positive, $-\lambda_n$, conj(λ_n) and conj($-\lambda_n$) are also the roots of eqn (19). We take λ_n and $-\lambda_n$ as roots and truncate an infinite number of roots at $n = N$. Consequently, the function ϕ_2^* is written in the form

$$\phi_2^* = \sum_{n=1}^{N} \{E_n e^{\lambda_n\psi} - \bar{E}_n e^{-\lambda_n\psi}\}\{Q(\lambda_n)J_0(\lambda_n\rho) + R(\lambda_n)\rho J_1(\lambda_n\rho)\}, \quad (20)$$

where

$$Q(\lambda_n) = 2(1 - \nu)J_1(\lambda_n) + \lambda_n J_0(\lambda_n), \tag{21a}$$

$$R(\lambda_n) = \lambda_n J_1(\lambda_n), \tag{21b}$$

and E_n and $\bar{E}_n$ are unknown complex coefficients.

The unknown complex coefficients are determined by the least squares method, so that the boundary condition (8b) may be satisfied at a number of midpoints (ρ_m, $m = 1, 2, \ldots, M$) across the top and bottom surfaces, this number being larger than N. Thus we obtain the simultaneous equations

$$\begin{vmatrix} \mathrm{Re}[X_{m,n}] & -\mathrm{Im}[X_{m,n}] & \mathrm{Re}[X_{m,n}] & -\mathrm{Im}[X_{m,n}] \\ \mathrm{Re}[e^{\lambda_n L}X_{m,n}] & -\mathrm{Im}[e^{\lambda_n L}X_{m,n}] & \mathrm{Re}[e^{-\lambda_n L}X_{m,n}] & -\mathrm{Im}[e^{-\lambda_n L}X_{m,n}] \\ \mathrm{Re}[Y_{m,n}] & -\mathrm{Im}[Y_{m,n}] & -\mathrm{Re}[Y_{m,n}] & \mathrm{Im}[Y_{m,n}] \\ \mathrm{Re}[e^{\lambda_n L}Y_{m,n}] & -\mathrm{Im}[e^{\lambda_n L}Y_{m,n}] & -\mathrm{Re}[e^{-\lambda_n L}Y_{m,n}] & \mathrm{Im}[e^{-\lambda_n L}Y_{m,n}] \end{vmatrix} \times \begin{vmatrix} \mathrm{Re}[E_n] \\ \mathrm{Im}[E_n] \\ \mathrm{Re}[\bar{E}_n] \\ \mathrm{Im}[\bar{E}_n] \end{vmatrix} = \begin{vmatrix} -\sigma^*_{0\psi\psi(\psi=0)} & -\sigma^*_{1\psi\psi(\psi=0)} \\ -\sigma^*_{0\psi\psi(\psi=L)} & -\sigma^*_{1\psi\psi(\psi=L)} \\ -\sigma^*_{0\rho\psi(\psi=0)} & -\sigma^*_{1\rho\psi(\psi=0)} \\ -\sigma^*_{0\rho\psi(\psi=L)} & -\sigma^*_{1\rho\psi(\psi=L)} \end{vmatrix}, \tag{22}$$

where

$$X_{m,n} = -Q(\lambda_n)\lambda_n^3 J_0(\lambda_n\rho_m) + R(\lambda_n)\{2(2 - \nu)\lambda_n^2 J_0(\lambda_n\rho_m) - \lambda_n^3\rho_m J_1(\lambda_n\rho_m)\}, \tag{23a}$$

$$Y_{m,n} = Q(\lambda_n)\lambda_n^3 J_1(\lambda_n\rho_m) - R(\lambda_n)\{2(1 - \nu)\lambda_n^2 J_1(\lambda_n\rho_m) + \lambda_n^3\rho_m J_0(\lambda_n\rho_m)\}. \tag{23b}$$

THERMAL AND RESIDUAL STRESSES

When the crystal is pulled a length ΔL, the temperature distribution changes from T^*_L to $T^*_{L+\Delta L}$, and the stress field also changes from $(\sigma^*_{ij})_L$ to $(\sigma^*_{ij})_{L+\Delta L}$. The stresses $(\sigma^*_{ij})_{L+\Delta L} - (\sigma^*_{ij})_L$ are stored in an arbitrary layer of $\zeta = \text{const}$. Consequently, the thermal stresses $(\sigma^*_{ij})^D$ at $\zeta = L_1$ during pulling when the crystal is pulled from L_1 to L are given by

$$(\sigma^*_{ij})^D = \int_{L_1}^{L} \left\{\frac{\partial(\sigma^*_{ij})_L}{\partial L}\right\} dL = (\sigma^*_{ij})_L - (\sigma^*_{ij})_{L_1}. \tag{24}$$

Equation (24) also shows that all stress components are zero at the interface, and no tractions are at the cylindrical surface and at the top end.

Moreover, when the crystal has been pulled out by the final length L_2 and attains very slowly to the uniform temperature $T^* = 0$, the residual stresses at $\zeta = L_1$ are given by

$$(\sigma^*_{ij})^A = (\sigma^*_{ij})^D - (\sigma^*_{ij})_{L_2}. \tag{25}$$

Putting $L = L_2$ in eqn (24) and substituting it in eqn (25), we have

$$(\sigma^*_{ij})^A = -(\sigma^*_{ij})_{L_1}. \tag{26}$$

With the usual technique of transformation of coordinates we find the three principal shearing stresses which act, respectively, on the mutually perpendicular planes.

We will discuss the stresses with the absolutely maximum principal shearing stresses, defined by $|\tau^*| = |\tau|(1 - \nu)/\{(T_m - T_a)\alpha E\}$, of three principal shearing stresses in the following section.

NUMERICAL RESULTS

The dimensionless parameters, i.e. the Biot number, the Peclet number and Poisson's ratio, are chosen as $B = 1$, $P = 0.02$ and $\nu = 0.3$ as typical values for large-diameter GaAs crystals. In order to compare with a semi-infinite crystal, we take $L_2 = 6$. This value is also used for Si. The infinite series in eqns (3), (9) and (12) are truncated at $n = 45$ so as to obtain an accuracy better than 0.5%. We chose $M = 21$ and $N = 19$ in eqn (22) so that the stresses $(\sigma^*_{\psi\psi})^D$ and $(\sigma^*_{\rho\psi})^D$ at the ends which must be zero may be less than 0.2% of $(\sigma^*_{\rho\rho})^D_{max}$ or $(\sigma^*_{\theta\theta})^D_{max}$.

Temperature distributions, axial distributions and radial distributions of stresses, respectively, are shown at the top [(1a)–(5a)], middle [(1b)–(5b)] and bottom [(1c)–(5c)] parts in Fig. 2. The first [(1a)–(1c)] to fifth [(5a)–(5c)] columns in the figure show the results of $L = 1.2$, 2, 4 and 6 during pulling and $L_2 = 6$ after pulling. The radial temperature gradient is always smaller than the axial one, but the former cannot be neglected in comparison with the latter. The temperature distribution near the solid–liquid interface is almost independent of L. For the case of $B = 0.01$ (for example, few-centimeters-diameter germanium crystals) the radial temperature gradient is negligible with respect to the axial one.

The stress distributions in the axial direction at $\rho = 0$ and $\rho = 1$ are shown at the middle in Fig. 2 because the extreme values of stress almost occur at these radial positions. The thermal stress at $\rho = 1$ increases rapidly to the peak value occurring at $\psi = 0.4$ and then decreases gradually. The position from the solid–liquid interface and the magnitude of the peak value are nearly equal [Fig. 2(1b)–Fig. 2(4b)]. It is found that the peak stresses at $\rho = 1$ and $\psi = 0.4$ is the maximum stress which the crystal undergoes during pulling. The thermal stress distribution from $\psi = 0$ to $\psi = 4$ when $L = 6$ [Fig. 2(4b)] is almost identical with one when $L = \infty$[8]. One of the most significant differences between the present model and the previous model of semi-infinite length is the thermal stress at $\rho = 0$ [Fig. 2(1b) and Fig. 2(2b)]. The peak thermal stress at $\rho = 0$ occurs at the top end of the crystal for $L < 2.4$, and it occurs at $\zeta = 2$ for $L > 2.4$. The peak stress at $\rho = 0$ has a maximum when $L = 1.2$, which attains about 40% of the maximum thermal stress at $\rho = 1$. If $B = 0.1$ and $B = 0.01$, it attains 63% and 66%, respectively. This result cannot be obtained from the model of semi-infinite length. This stress may lead to the formation of dislocations observed at the core of the crystal.

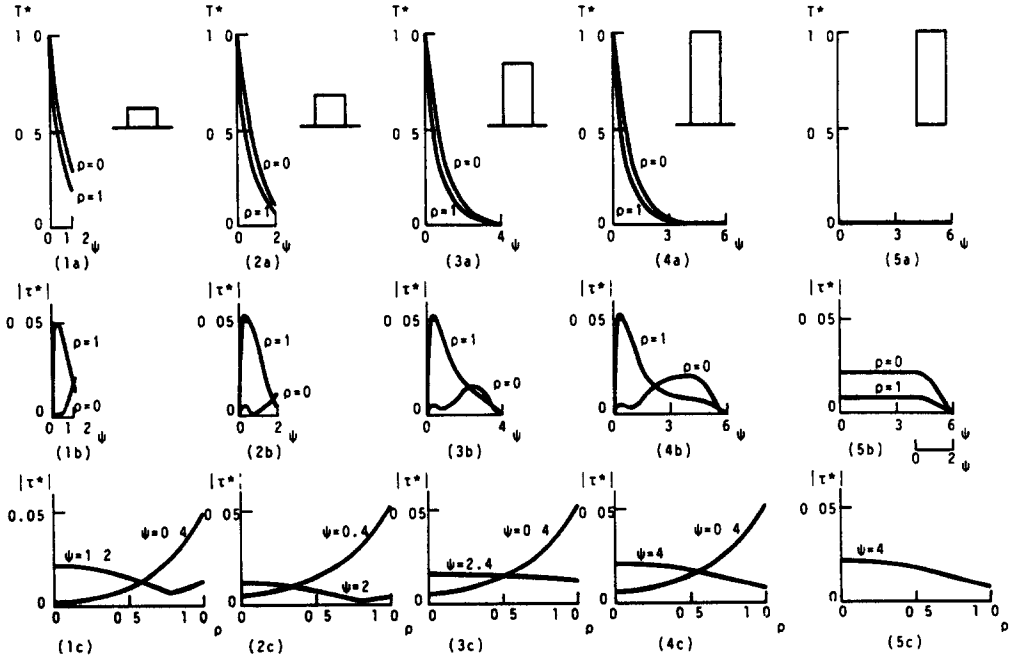

Fig. 2 Temperature and stress distributions

The radial distributions of the stress are illustrated at the bottom of Fig. 2. The sharp breaks in the curves for $\psi = 1.2$ in Fig. 2(1c) and $\psi = 2$ in Fig. 2(2c) are due to the change of the slide plane in which $|\tau^*|$ occurs. A considerably higher thermal stress occurs at the periphery near the solid–liquid interface. Near the top end the stress at the core is greater than that at the periphery except for the middle stage of pulling [Fig. 2(3c)]. We can read the residual stresses for the case of $L_2 < 6$ from Fig. 2(5b). Then, the origin of the abscissa is moved to $\psi = 6 - L_2$, as shown under the figure; the lower abscissa shows the case of $L_2 = 2$ as an example. As described in ref. [8], we can estimate qualitatively the dislocated regions from the elastic stress distributions. Because dislocations are produced by shearing stress, it can be expected that a high dislocation density region is present near the periphery and that a low dislocation density region is between the core and the periphery in the crystal. This estimation agrees with the experimental results obtained by Jordan *et al.*[7], Shimada *et al.*[9] and Chen and Holmes[10].

Figure 3 shows the dependence of the maximum thermal stress and residual stress on the Biot number. The plotted points represent the crystal of a finite length $L_2 = 10$ (present model). The curves represent the crystal of a semi-infinite length and are quoted from ref. [8]. Here, the numerical errors of ref. [8] are corrected. It is found that the thermal and residual stresses are strongly affected by the Biot number. As the Biot number decreases, the temperature gradient of the crystal reduces, and the stresses also decrease. Shimada *et al.*[9] succeeded in growing crystals with a low and homogeneous dislocation density by the reduction of the temperature gradient. This experimental result can be explained by Fig. 3. The highest thermal stress occurs at $\rho = 1$ for both models. Therefore, a part of the conclusion in ref. [8] that the maximum stress occurs at the center of the crystal for large values of the Biot number should be corrected. The maximum thermal stress at $\rho = 0$ which is produced at the early stage of the pulling ($L < 2$) is always greater than the residual stresses after pulling. For small values of the Biot number, higher stresses are obtained for a finite crystal than for an infinite crystal. This means that the high thermal stress is produced during the early stage of the pulling. On the contrary, for large values of the Biot number, a high stress

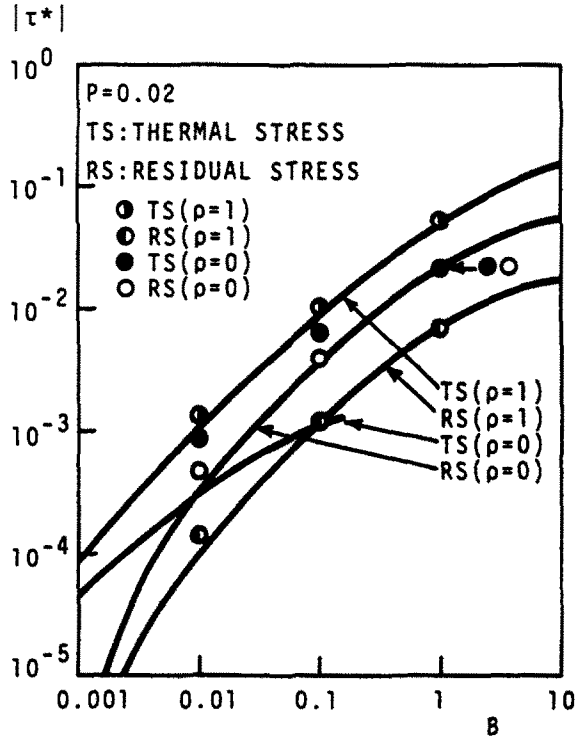

Fig. 3. Maximum thermal stress and residual stress vs Biot number.

is produced near the solid–liquid interface and is independent of the crystal length if the QSS assumption is satisfied.

CONCLUSIONS

1. The thermal stress during pulling and the residual stress after pulling are affected strongly by the Biot number.

2. The highest thermal stress is produced at the periphery in the crystal.

3. When $P = 0.02$, the thermal stress near the solid–liquid interface is almost independent of the crystal length for the large Biot number, and it depends on the crystal length for the small Biot number.

REFERENCES

1. N. Kobayashi, In *Preparation and Properties of Solid State Materials* (Edited by W R Wilcox), Vol 6 Marcel Dekker, New York (1981).
2. E. Billig. Some defects in crystals grown from the melt (1. Defects caused by thermal stresses) *Proc Roy. Soc* **A235**, 37–55 (1956).
3. S. A. Tsivinsky, Dislocation density in pure crystals grown from melts *Kristall und Technik* **10**, 5–35 (1975).
4. P Penning, Generation of imperfections in germanium crystals by thermal strain. *Philips Res Repts* **13**, 79–97 (1958)
5. N. A. Avdonin, S. S. Vakhrameev, M. G. Mil'vidskii, V. B. Osvenskii, B A. Sakhavov, V A Smirnov and Yu. F. Shchelkin, Influence of the temperature field and the thermal stress field upon the formation of the dislocation structure in gallium-arsenide single crystals grown by the Czochralski method. *Soviet Phys.-Dokl.* **16**, 772–775 (1972).
6. J. C. Brice, The cracking of Czochralski-grown crystals *J Crystal Growth* **42**, 427–430 (1977)
7. A S. Jordan, R. Caruso and A. R. Von Neida, A thermoelastic analysis of dislocation generation in pulled GaAs crystals. *Bell System Tech. J.* **59**, 593–637 (1980)
8. T Iwaki and N Kobayashi, Residual stresses of Czochralski-grown crystal *ASME J. Appl Mech* **48**, 866–870 (1981).
9. T. Shimada, K. Terashima, H. Nakajima and T. Fukuda, Growth of low and homogeneous dislocation density GaAs crystal by improved LEC technique. *Jap. J. Appl. Phys.* **23**, L23–L25 (1984)
10. R T Chen and D. E. Holmes, Dislocation studies in 3-inch diameter liquid encapsulated Czochralski GaAs *J Crystal Growth* **61**, 111–124 (1983).